Cartilage
2015, Vol. 6(3) 174–184

DOI: 10.1177/1947603515572874
cart.sagepub.com
SAGE

Monitoring the Progression of Spontaneous Articular Cartilage Healing with Infrared Spectroscopy

Megan P. O'Brien[1], Madhuri Penmatsa[1], Uday Palukuru[1], Paul West[3], Xu Yang[2], Mathias P. G. Bostrom[2], Theresa Freeman[4], and Nancy Pleshko[1]

Abstract

Objective. Evaluation of early compositional changes in healing articular cartilage is critical for understanding tissue repair and for therapeutic decision-making. Fourier transform infrared imaging spectroscopy (FT-IRIS) can be used to assess the molecular composition of harvested repair tissue. Furthermore, use of an infrared fiber-optic probe (IFOP) has the potential for translation to a clinical setting to provide molecular information *in situ*. In the current study, we determined the feasibility of IFOP assessment of cartilage repair tissue in a rabbit model, and assessed correlations with gold-standard histology. *Design*. Bilateral osteochondral defects were generated in mature white New Zealand rabbits, and IFOP data obtained from defect and adjacent regions at 2, 4, 6, 8, 12, and 16 weeks postsurgery. Tissues were assessed histologically using the modified O'Driscoll score, by FT-IRIS, and by partial least squares (PLS) modeling of IFOP spectra. *Results*. The FT-IRIS parameters of collagen content, proteoglycan content, and collagen index correlated significantly with modified O'Driscoll score (P = 0.05, 0.002, and 0.02, respectively), indicative of their sensitivity to tissue healing. Repair tissue IFOP spectra were distinguished from normal tissue IFOP spectra in all samples by PLS analysis. However, the PLS model for prediction of histological score had a high prediction error, which was attributed to the spectral information being acquired from the tissue surface only. *Conclusion*. The strong correlations between FT-IRIS data and histological score support further development of the IFOP technique for clinical applications, although further studies to optimize data collection from the full sample depths are required.

Keywords

cartilage, repair tissue, infrared fiber-optic probe, FTIR spectroscopy

Introduction

Accurate assessment of the progression of cartilage healing is necessary to improve treatment for degenerative articular cartilage. Currently, animal models such as chondral and osteochondral defects in rabbits, goats, dogs, and sheep are used to develop treatment techniques for optimizing repair.[1-6] Osteochondral repair is associated with a series of physiological changes, including localized bleeding, hematoma formation, stem cell migration, and the activity of growth factors that influence the chondrocyte-like cell formation. In both preclinical and clinical healing, these procedures unfortunately often result in formation of type I collagen containing fibrocartilage, which is mechanically inferior to the desired type II containing hyaline cartilage.[7-10]

To assess the quality of the various treatments in animal models, methods for monitoring progression of repair are necessary. Current assessment techniques are typically invasive and destructive, requiring tissue harvesting to perform, for example, immunohistochemical and histological staining.[11-13] This is becuase of the fact that to date, assessment by histological staining is not only the best but the only truly accurate method to identify structural and compositional changes in cartilage.[14] Histological assessments of cartilage are performed through the use of quantitative scoring systems such as the modified O'Driscoll score.[15,16] This subjective score requires the observer to rate different aspects of the repair tissue based on, for example, integration, hypocellularity, adjacent tissue degererative changes,

[1]Department of Bioengineering, Temple University, Philadelphia, PA, USA
[2]Hospital of Special Surgery; New York, NY, USA
[3]Department of Mathematics, Engineering & Computer Science, LaGuardia Community College, Long Island City, NY, USA
[4]Department of Orthopaedics, Thomas Jefferson University, Philadelphia, PA, USA

Corresponding Author:
Nancy Pleshko, Department of Bioengineering, Temple University, 1947 North 12th Street, Philadelphia, PA 19122, USA.
Email: npleshko@temple.edu

and proteoglycan (PG) staining, where tissues more closely resembling true hyaline cartilage receive a higher score. Although currently the gold standard, there are several drawbacks to the use of histological scoring systems in general, including time consumption, variability in tissue staining, subjective analysis (leading to large interobserver variability),[17,18] the inability to translate to *in vivo* applications, and insufficient molecular correlations.[19]

Fourier transform infrared imaging spectroscopy (FT-IRIS) is an alternative method for the evaluation of structural and compositional variations in cartilage based on molecular information.[20-23] This semiquantitative method provides information that is not subjective, and therefore does not rely on interobserver agreement. Recent FT-IRIS studies on cartilage have investigated a variety of disease states and effects of mechanical stress, and have found tissue changes associated with the effect of mechanical compression on articular cartilage components,[24] in cartilage in a mouse model of rheumatoid arthritis,[25] in tracheal cartilage in neonatal lambs associated with mechanical ventilation,[26] between normal and repair cartilage in rabbits,[27] and between cartilage of different species.[28] In our laboratory, most recently we have used FT-IRIS to investigate human osteoarthritis and the composition of cartilage repair tissue[29,30] to differentiate collagen types in cartilage and meniscus,[31] to evaluate tissue engineered and degraded cartilage for comparison with magnetic resonance imaging parameters,[32,33] and in rabbit models, to evaluate new repair tissue formation,[34] and compare biochemical crosslink analysis to FT-IRIS parameters in the same rabbit model as is evaluated in this study.[35]

Here, we report FT-IRIS parameters, which we correlate with histologic evaluation of the progression of cartilage repair over time in a rabbit osteochondral defect model. This lays the groundwork to demonstrate the sensitivity of FT-IRIS parameters to monitor tissue healing. Furthermore, the potential of using an infrared fiber optic probe (IFOP) for minimally invasive clinical assessment was investigated. Recent IFOP studies of human cartilage have shown the ability to monitor cartilage degradation and demonstrated correlations with osteoarthritic tissue grade,[29,36] but to date there has been no data that shows discrimination between repair and normal tissue in intact tissues using mid-infrared fiber-optic spectroscopic analysis.

Methods

Cartilage Defect Model

Bilateral full thickness osteochondral defects 3 mm in diameter and ~2.5 mm deep were created in the hind legs of 28 mature New Zealand white rabbits under an Institutional Animal Care and Use Committee (IACUC)–approved protocol from the Hospital for Special Surgery, New York, USA. Animals were sacrificed using barbiturate overdose at 2 ($n = 4$), 4 ($n = 4$), 6 ($n = 5$), 8 ($n = 5$), 12 ($n = 5$), and 16 ($n = 5$) weeks post–defect creation. At each time point, the defect and adjacent tissue were sampled by the IFOP (details below), and the tissues harvested for histology and FT-IRIS.

Tissue Preparation

Tissues were fixed in formalin, decalcified, and processed for paraffin embedding. Tissues were then sectioned perpendicular to the articular surface for infrared imaging (7 μm thickness) and histology (6 μm thickness). Tissues for FT-IRIS were mounted onto low-e slides (Kevley Technologies, Chesterland, OH), and for histology, mounted onto plus slides. Tissue sections were deparaffinized prior to analysis using xylene and varying grades of ethanol washes.

Infrared Fiber Optic Probe Data Collection

An IFOP was used for spectral data collection from the intact knees prior to tissue harvest as previously described.[36] The IFOP consists of a flexible fiber-optic bundle that contains chalcogenide glass that transmits over the infrared spectral region of 4000 to 900 cm^{-1} (Remspec Corp, Sturbridge, MA). The fiber bundle was coupled to a Bruker spectrometer (Billerica, MA) equipped with a mercury cadmium telluride (MCT) detector module. The bundle is coupled on the other end to a ZnS attenuated total reflectance (ATR) crystal with a flat tip roughly 1 mm in diameter. A 5-pound load cell (Omega Engineering Series LCFA-5, Stamford, CT) was used to maintain the crystal tip of the IFOP bundle in contact with the sample at a controlled pressure of 0.7 pounds, as described previously in West *et al*.[37] Spectra were collected with 8 cm^{-1} spectral resolution after allowing the tissue to relax around the crystal tip of the apparatus for ~60 seconds.

Spectra were obtained in triplicate from visually identified repair and adjacent normal regions for each knee. As a secondary goal of this study was to determine how to optimize the contact between the fiber optic probe and the repair tissue, many spectra that were collected initially were not usable due to inadequate contact. Ultimately, 69 spectra were used for analysis. Of the 69 spectra, 25 were obtained from animals sacrificed at 2 weeks postsurgery, 15 from animals sacrificed 6 weeks postsurgery, 23 from animals sacrificed 12 weeks postsurgery, and 6 from animals sacrificed 16 weeks postsurgery. Regions of interest for typical cartilage peaks were initially determined in an earlier study (**Fig. 1A**)[23] and are elaborated on in the FT-IRIS section.

Histology

Histological sections were stained with Alcian blue and hematoxylin and eosin, where dark blue reflects proteoglycan (PG) amount, red and pink are representative of nuclei, and a pale pink is associated with the cytoplasm.

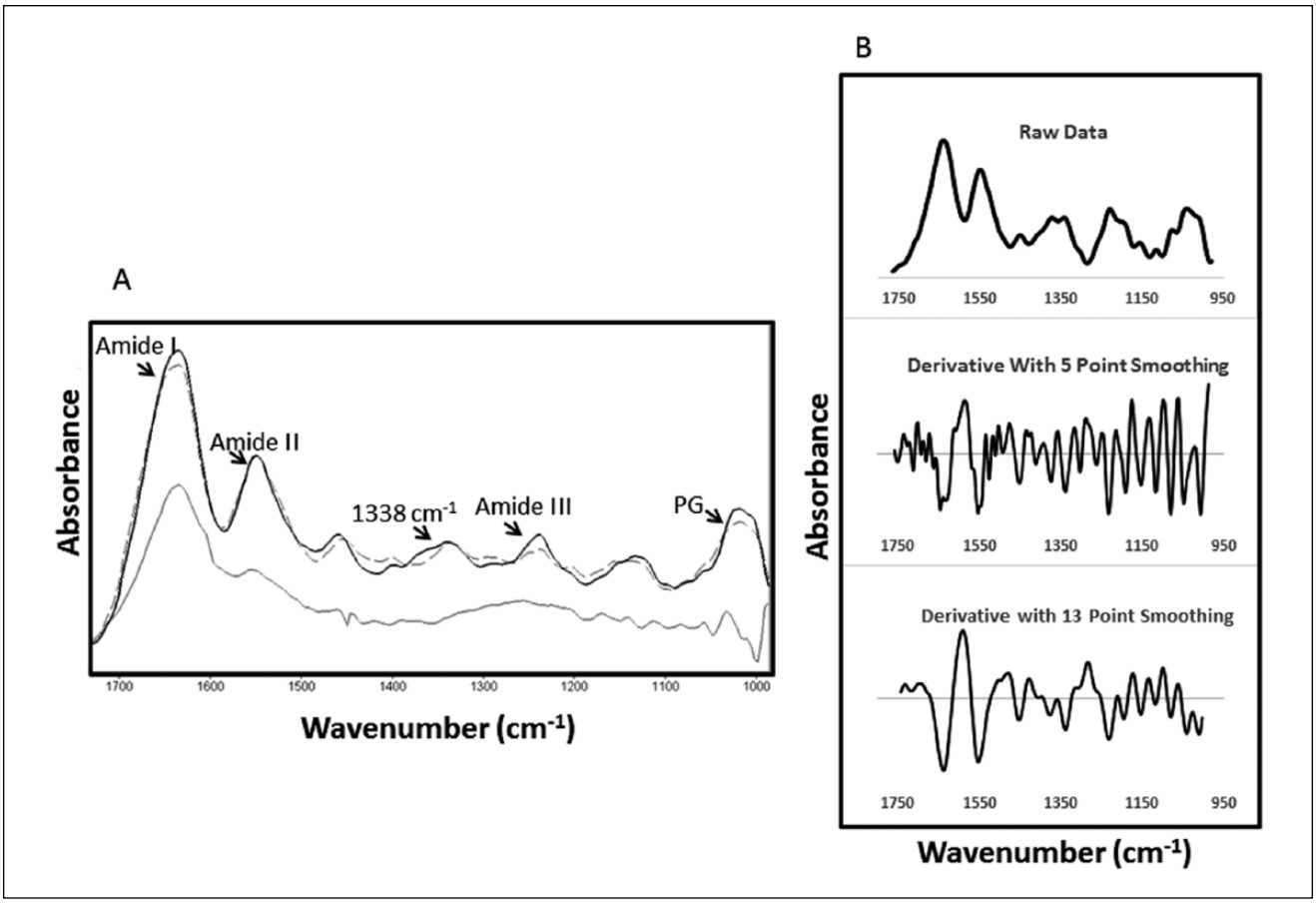

Figure 1. (**A**) Repair (gray lines) and normal (solid dark line) infrared fiber optic spectra collected from rabbit cartilage. The dashed gray line is taken from 8 weeks postsurgery, while the solid gray line was taken from 2 weeks postsurgery. There was a progression in the repair spectra toward a more normal spectrum with increasing time postsurgery. The peaks of interest are labeled, with amide peaks reflecting protein absorbances, PG reflecting proteoglycan sugar absorbances, and the 1338 cm^{-1} peak from collagen. (**B**) Raw spectra (top), second derivative spectra with little smoothing, where noise is still evident (middle), and after a Savitzky Golay third-degree 13-point smoothing algorithm was applied (bottom). The 13-point smoothed spectra were used in the partial least squares (PLS) model.

Hematoxylin and eosin stains the nuclei blue and cytoplasm and extracellular matrix pink.[38]

Stained sections of cartilage repair tissue were scored by 2 blinded independent observers using the modified O'Driscoll semiquantitative scoring system.[15] This scoring system ranges from 0 to 24 with 24 being hyaline-like cartilage, and 0 representing no repair cartilage present. Parameters include the 4 main categories of nature of predominant tissue (which includes cell morphology and PG staining, structural characteristics (which includes structural integrity features and bonding to adjacent cartilage), freedom from cellular changes of degeneration (which includes features of hypocellularity and clustering), and freedom from degenerative changes in adjacent tissue (which includes cellular morphology and hypocellularity features). Structural integrity is a measure of how intact the sample is histologically below the surface. PG staining (in our case using Alcian blue) reflects the quality of staining for PG content throughout the cartilage region. Hypocellularity reflects the amount of cells present throughout the tissue, with increasing hypocellularity related to unhealthy tissue. Agreement between the independent graders was determined by a kappa calculator.[39]

Fourier Transform Infrared Imaging Spectroscopy

FT-IRIS data were obtained using a Perkin Elmer Spectrum Spotlight 400 imaging spectrometer (Perkin Elmer, Shelton, CT). A rectangular region of interest was selected that contained the defect and adjacent normal cartilage. Data were acquired in the mid IR range (4000 to 700 cm^{-1}) in imaging mode at a pixel resolution of 25 μm and spectral resolution of 8 cm^{-1}.

Table 1. Ranges for Variables Used to Calculate Sensitivity and Specificity of Prediction of Tissue Type by Fiber-Optic Probe Spectra.

Variable	Definition	Range
True positive	Repair tissue predicted to be repair tissue	0.6 to 1.4
True negative	Normal tissue predicted to be normal tissue	−0.6 to 0.5
False positive	Normal tissue predicted to be repair tissue	0.6 to 1.4
False negative	Repair tissue predicted to be normal tissue	−0.6 to 0.5

Polarized experiments were done to qualitatively assess collagen orientation by insertion of a wire grid polarizer in the beam path angled at 0°.[40] Assessment of the ratio of the amide I/amide II absorbance yields information on fibril orientation where a ratio ≥2.7 reflects fibrils aligned parallel to the articular surface, a ratio ≤1.7 reflects fibrils perpendicular to the articular surface and a ratio between 2.7 and 1.7, reflects a random or mixed fibril orientation.[40,41]

Imaging data for repair and normal cartilage were analyzed using ISyS 5.0 software (Malvern, UK). The spectral region from ~900 to 2000 cm^{-1} was considered as it has been shown to contain molecular information that arises from collagen and PG, the primary components of cartilage,[20,22,23,42,43] The peaks of interest were the integrated areas of 1594 to 1718 cm^{-1}(amide I − total protein quantity) and 958 to 1144 cm^{-1} (correlated to PG quantity).[43] It was assumed that the amide I absorbance arises primarily from collagen. The integrated area of the 1338 cm^{-1} absorbance (that arises from collagen) ratioed to the amide II absorbance has previously been shown to reflect changes in type II collagen helical integrity,[44] or to collagen type in mixed hyaline and fibrocartilage based on immunohisto-chemistry studies.[30] Given that mixed collagen types are present in the current data set, here, we report this parameter as "collagen index," where it is related to the relative amounts of collagen I and collagen II, with higher values indicative of more collagen type II.

Cartilage sections were divided into normal, adjacent normal, and defect repair tissue. The defect region was differentiated based on its surface features, PG content, and collagen orientation. The region just next to the repair tissue and close to normal tissue was considered the adjacent normal region, and was excluded from quantitative analyses. Average values for parameters were obtained from regions of repair and from normal cartilage away from the defect tissue for each section.

Chemometric Model

Partial least squares (PLS) is a chemometric method used to generate predictive models for highly collinear data with many factors.[45] In general, PLS extracts latent factors from the data that account for the most variation within the responses. Using these factors, a model is generated for predicting responses. Two PLS models were generated using the IFOP spectra in Unscrambler X (CAMO Software, Oslo, Norway). In a previous study, a PLS model based on human cartilage was developed that used a specified region of the spectra, 1733 to 984 cm^{-1}.[36] This region was used again for both models, with the exclusion of 1404 cm to 1500 cm^{-1} due to spectral artifacts that were present in the majority of the spectra.

The first PLS model used all 69 spectra and was built to distinguish repair from normal tissue. Several preprocessing algorithms were investigated to optimize the model, and ultimately, the best outcome was found using second derivative preprocessing with the Savitzky Golay method with a degree of 3 and 13 point smoothing (sample spectra shown in **Fig. 1B**). Validation was done using a full leave one out cross-validation (as described in Padalkar *et al*.[46]), and the quality of the model was determined by the root mean square error (RMSE) values of the model and validation,[46] and by specificity and sensitivity measurements.

To calculate specificity and sensitivity, repair tissue was assigned a value of "1" and normal cartilage a value of "0." Ranges were defined for true positives, true negatives, false positives, and false negatives (**Table 1**).

After finding the number of samples that fell into each category, sensitivity and specificity were calculated using Equations (1) and (2).[47]

$$\text{Sensitivity} = \text{True positives}/\left(\text{True positives} + \text{False Negatives}\right) \quad (1)$$

$$\text{Specificity} = \text{True Negatives}\ /\left(\text{True Negatives} + \text{False Positives}\right) \quad (2)$$

Following the same methodology, a second PLS model was used to predict the modified O'Driscoll score of the samples. Histological scores were only completed for samples acquired from the right knees of the animals (as tissues from the left knees were used for destructive compositional analyses.[48] This resulted in the use of 57 spectra for this model (19 spectra from 2 weeks postsurgery; 12 from 6 weeks postsurgery; 20 from 12 weeks postsurgery; and 6 from 16 weeks postsurgery). Preprocessing consisted of taking the first derivative using the Savitzky-Golay method with a degree of 2 and 13-point smoothing, and validation done with a full

leave one out cross validation. The input for this model had responses that ranged from 6 to 24 for the modified O'Driscoll score. The model quality was assessed by the RMSE values of the model calibration and validation.

Statistical Evaluation

Means and standard deviations were calculated for the FT-IRIS parameters of collagen index, and collagen and PG content. For each group, a paired Student *t* test was used to compare values of normal and repair parameters. To determine differences among repair tissue parameters for the 6 different time points, a one-way analysis of variance (ANOVA) (SigmaStat 3.1, Systat Software Inc., San Jose, CA) was used followed by a *post hoc* comparison using Tukey's test with significance set at an overall P value <0.05. A two-way ANOVA was used for all pairwise comparisons with time point and tissue type as factors, and Bonferroni's test used for *post hoc* comparisons. FT-IRIS parameters of repair tissue were then compared to the modified O'Driscoll score using a Pearson correlation, with $P < 0.05$ considered significant. FT-IRIS parameters obtained from repair tissue were also compared with the individual components of the modified O'Driscoll score to ascertain which specific aspects of tissue quality related to FT-IRIS–determined parameters.

Results

Histological Grading

Agreement between the independent graders had a kappa statistic value of 0.81, which corresponds to nearly perfect agreement.[39] An overall increasing trend was observed in the modified O'Driscoll scores for the repair tissue over time with the exception of week 12 postsurgery (**Fig. 2**). The O'Driscoll score was significantly greater at week 16, compared with weeks 2 and 8. There was an overall improvement in the fill of the defect and quality of the tissue over time as shown from the histological scores. The nature of the predominant tissue was hyaline in only ~12% of all the samples (3/25), and fibrocartilage for ~60% of the samples. Of the 12% containing a hyaline-like cartilage, 67% were samples from the week 16 time point. The other sample comprising this group was a 4-week sample. The remaining ~28% was categorized as fibrous tissue. The surface regularity was smooth and intact in 24% of the samples. Approximately 12% of the samples had normal proteoglycan staining (2 samples from week 16 and 1 sample from week 4) and 57% of all samples were bonded to adjacent cartilage at both ends.

Fourier Transform Infrared Imaging Spectroscopy Analysis

Comparison of histological staining with FT-IRIS derived images shows similar changes in the repair cartilage with increasing time postsurgery (**Fig. 3**). Based on histological scores and spectral parameters, it is evident that the defect region was filled with repair tissue at 8 weeks in most of the samples. Qualitatively, most of the samples demonstrated higher PG content in normal articular cartilage relative to the repair tissue. For the majority of samples, there was no obvious orientation of repair tissue as is typically seen in hyaline cartilage, except in the 16-week samples with predominantly hyaline cartilage.

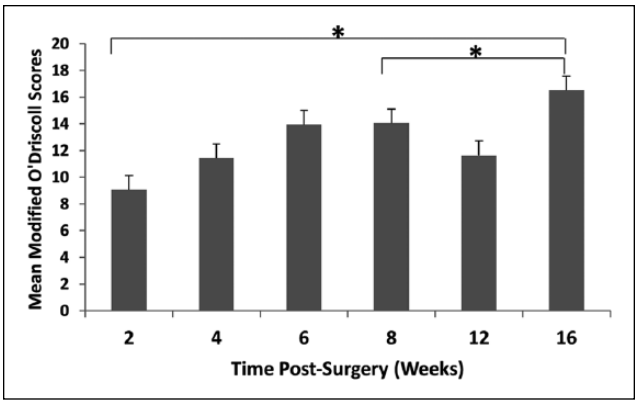

Figure 2. A trend for increasing modified O'Driscoll score was observed with increasing time postsurgery (excluding week 12). *Significantly different at $P < 0.05$.

Collagen Content

Initially, collagen content in the repair tissue was lower than normal tissue, but increased to near-normal values by 8 weeks postdefect creation (**Fig. 4**). Significantly higher repair tissue collagen content was found at weeks 12 and 16 compared with week 6 postsurgery (**Fig. 4**).

Proteoglycan Content

Proteoglycan followed a similar trend as collagen content; in the repair tissue, an initial lower than normal value was observed that increased over time. The PG content was significantly lower for the repair tissue relative to the normal tissue for weeks 2, 6, and 8 postsurgery. The amount of PG increased significantly from week 6 to week 16 postsurgery (**Fig. 4**), but averages never reached the levels found in the normal articular cartilage. Similar to collagen content, the results indicate a significant improvement beginning at 8 weeks in most of the samples.

Collagen Index

The collagen index was initially lower at the first 3 time points (more type I collagen), and increased to closer to normal values by the 8-week time point. It was also significantly lower for the repair groups relative to normal for

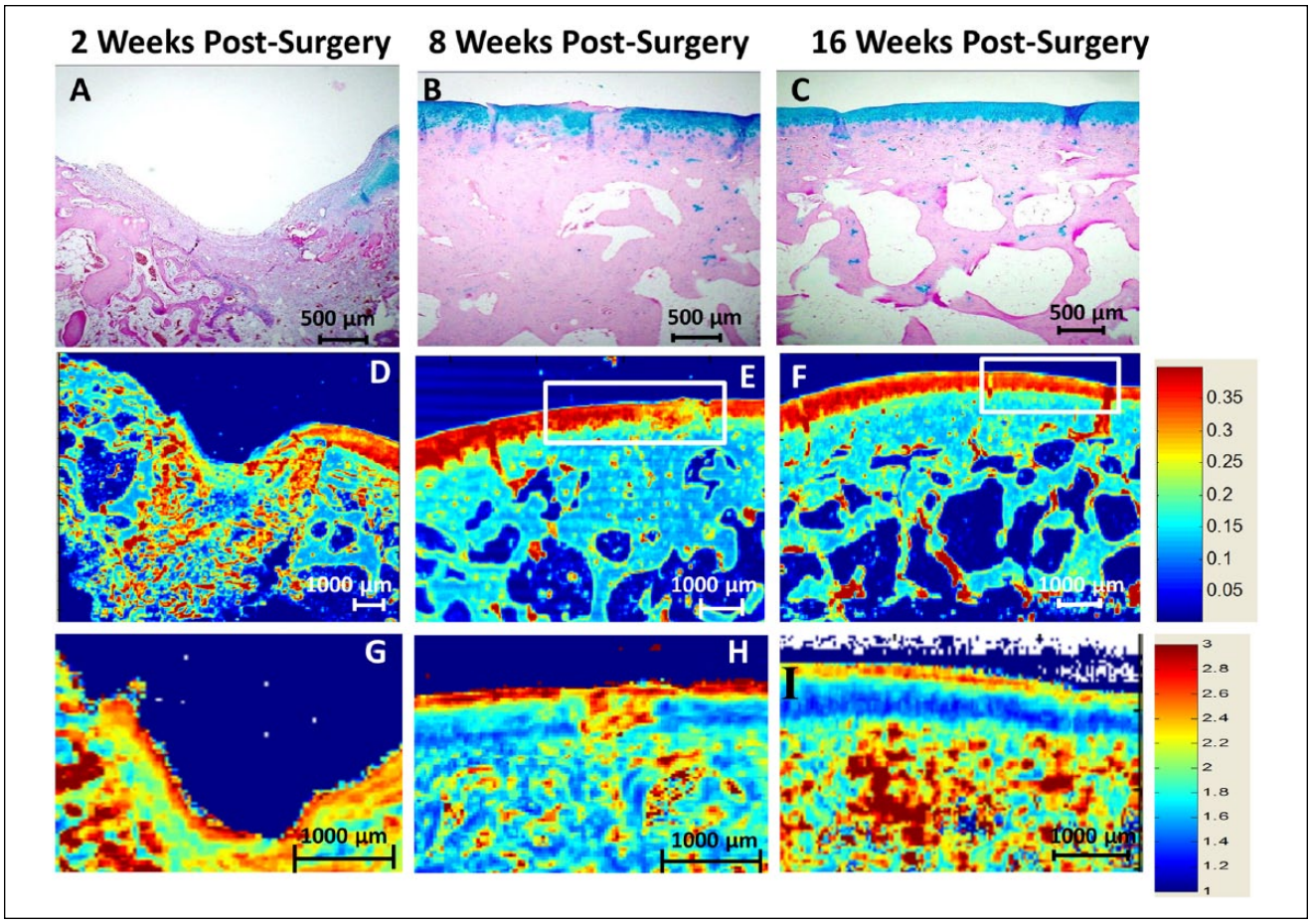

Figure 3. Images of samples stained with Alcian blue, hematoxylin and eosin (**A**, **B**, and **C**), and Fourier transform infrared imaging spectroscopy (FT-IRIS)–derived images (**D**, **E**, and **F**) of proteoglycan (PG) content for 2, 8, and 16 weeks postsurgery. (**G**, **H**, and **I**) Polarized images of the samples. The white box indicates the region displayed in the histology images. Qualitatively, tissue fills increases with time, as does PG content. Zonal fiber orientation can be observed in the normal cartilage, but not in the earlier stages of repair tissue.

weeks 2, 4, and 6 postsurgery, and compared with the week 8 repair values (**Fig. 4**). The 12- and 16-week repair tissue had a significantly higher index (more type II collagen) compared with the 4-week repair tissue.

Correlations

Significant correlations were found between the overall modified O'Driscoll score and the FT-IRIS repair parameters of collagen quantity, collagen index, and PG with P values of 0.05, 0.02, and 0.002, respectively. These 3 FT-IRIS parameters also correlated with individual components of the O'Driscoll score. Collagen quantity was related to the Alcian blue staining, structural integrity, and freedom from degenerative changes in the adjacent tissue ($P = 0.005$, 0.04, and 0.05, respectively). PG quantity significantly correlated with the nature of the predominant tissue, Alcian blue staining, and hypocellularity ($P = 0.02$, 0.003, and 0.46, respectively). Collagen index correlated with Alcian blue staining and hypocellularity ($P = 0.05$ and 0.05, respectively).

Infrared Fiber Optic Probe Analysis

The PLS model for distinguishing repair and normal cartilage was able to completely discriminate these tissue types, with a sensitivity and specificity of 1.0. The RMSE of calibration value for the best PLS model for prediction of modified O'Driscoll score was 1.70 using the optimal number of factors, 5, and the RMSE of validation was 3.59 (**Table 2**). These prediction errors are too high to be practically useful for scoring of tissues on a scale of 24.

Discussion

As has been previously demonstrated, FT-IRIS is a powerful method for assessment of repair tissue composition.[34,42] Earlier studies show how FT-IRIS can distinguish repair

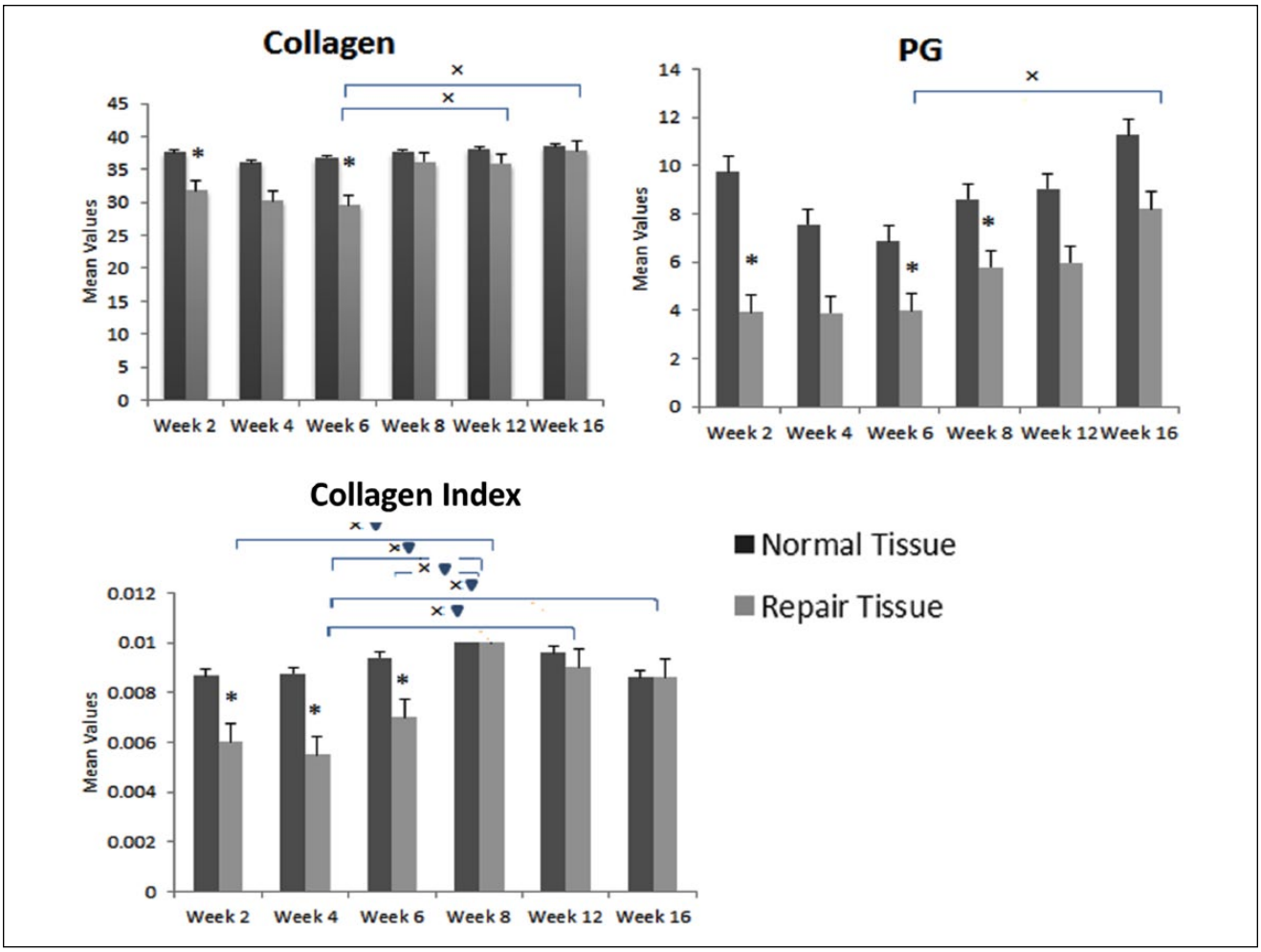

Figure 4. Fourier transform infrared imaging spectroscopy (FT-IRIS) parameters of repair and normal tissue. Significant differences were assessed by one-way analysis of variance (ANOVA) among all 6 groups ($P < 0.05$ represented by "×") for repair tissue at different time points. A paired Student *t* test was used to compare the normal and repair values within each group (*). A two-way ANOVA was used for pairwise comparisons with time point and conditions as factors, with Bonferroni's test used for *post hoc* comparisons (▼).

Table 2. Summary of the IFOP PLS Models and Corresponding Validations (PLS Full Cross-Validation Method) from Repair and Normal Cartilage of Rabbit Knees.

Method		No. of Spectra	Preprocessing	RMSE Value	Regression Coefficient (R^2)	Sensitivity/ Specificity
PLS model for distinguishing repair samples from normal samples	Model	69	Savitzky-Golay 2nd derivative (3rd degree, 13-point smoothing)	0.11	0.94	Sensitivity = 1.0
	Validation	69		0.16	0.88	Specificity = 1.0
PLS model for predicting the O'Driscoll scores	Model	57	Savitzky-Golay 1st derivative (2nd degree, 13-point smoothing)	1.7	0.91	NA
	Validation	57		3.59	0.60	

IFOP = infrared fiber optic probe; PLS = partial least squares; RMSE = root mean square error.

and normal tissue composition[42] and that progressive changes in several FT-IRIS parameters occur when monitoring a rabbit model of short-term cartilage repair (3 and 6 weeks).[34] Important advances over the previous studies include demonstration of the progression of FT-IRIS parameters over a longer repair period (16 weeks), and correlation

of FT-IRIS parameters, including the collagen index related to collagen type, with gold-standard histological grading. The importance of this finding is twofold; the capability of FT-IRIS to provide reliable semiquantitative measurements, and the potential to translate the spectroscopic data to an *in vivo* assessment, the latter not possible with histological staining.

Semiquantitative histological assessment of cartilage has also been performed previously, including a study by Julkunen *et al*.[49] in 2009 where Safranin-O–stained histological sections were assessed by digital densitometry for PG quantification.[49] As in FT-IRIS analysis, loss of carbohydrates during the fixation process must be minimized, and as a result, some conventional fixation and processing methods cannot be used.[50] In addition, metachromatic staining may occur, which can complicate the use of this methodology to quantify PGs, since the stain may then have more than one maximum absorption value.[50] The use of semiquantitative FT-IRIS parameters also has certain limitations, including the need to evaluate which specific parameter for PG content will yield the most accurate results.[28] In the current study, the use of the integrated area of the PG absorbance showed significant correlation with the Alcian blue staining component of the modified O'Driscoll score, indicative of the appropriateness of this parameter. It is also important to note that there was high agreement between O'Driscoll score graders in the current study, likely because of having the graders trained together, which is clearly an ideal case. Without the combined training, it is possible that there would have been higher interobserver variability due to the subjective nature of the score.[51] However, a recent study that compared interobserver and intraobserver reliability of 5 different cartilage scoring systems also found quite high reliability among 3 graders.[52]

FT-IRIS analysis also showed that significant changes in repair tissue parameters over time were attributable to a combination of collagen parameters (collagen content and type), in addition to PG. Significant correlations of collagen content, collagen type (index), and PG with the overall modified O'Driscoll score support this as well. Using FT-IRIS data, however, 1 image can be acquired and assessed for the 3 FT-IRIS parameters, while for the histological grading, nine categories are graded by multiple graders. The correlations of the FT-IRIS parameters and histological scoring categories imply that FT-IRIS may be a more succinct, less subjective, method to obtain information similar to that obtained from staining.

The parameters from the modified O'Driscoll score that correlated significantly or nearly significantly with FT-IRIS parameters included structural integrity, Alcian blue staining, nature of the predominant tissue, hypocellularity, and freedom of degenerative changes in adjacent tissue. It is interesting to think about how the FT-IRIS–derived parameters can reflect the seemingly diverse histological parameters.

All three FT-IRIS parameters correlated with Alcian blue staining, with the relationship between PG and Alcian blue staining expected. The positive correlation with collagen index is also not surprising, as a higher collagen index indicates more type II collagen, and the greater the amount of type II collagen, the greater PG we would expect. However, since collagen content increased over time, and is not necessarily dependent on a corresponding increase in PG, the correlation with Alcian blue staining might not reflect a direct relationship. Additionally, the correlation of FT-IRIS PG content with the nature of the predominant tissue is also not surprising, given that there should be more PG content in hyaline cartilage as compared with fibrocartilage.

A significant correlation was also observed between PG and (less) hypocellularity. Less hypocellularity indicates healthier tissue, with greater chondrocyte activity, findings that would also support greater PG content. Collagen content also correlated with structural integrity and lack of degenerative changes in adjacent tissue values, a parameter related primarily to cellularity features. It seems likely that increased collagen content would improve structural integrity, and enable improved integration with surrounding tissue, a finding observed in other studies.[53,54]

Despite the strong correlations of FT-IRIS data with O'Driscoll score, use of either of these methods is not possible on intact tissue, or *in situ*. *In situ* evaluation of repair tissue in animal models has been performed with magnetic resonance imaging (MRI) studies, where several different MR parameters have been investigated.[55] Watrin-Pinzano *et al*.[56] used MRI T2-mapping to quantitatively assess repair cartilage in a rat patella model. The authors demonstrated the ability to obtain T2 measurements showing the zonal variation observed in animal cartilage, which have previously been correlated to collagen network organization.[57] However, as molecular composition information was not obtained, it is not clear which specific attributes of the cartilage structure actually contributed to the T2 zonal variations. In our study by Kim *et al.*,[34] we directly compared FT-IRIS and MRI parameters obtained from early stage osteochondral repair tissue in rabbits. We found a significant inverse correlation between the T2 relaxation data and FT-IRIS–determined collagen orientation in the normal cartilage, but no significant correlations between T2 relaxation values and FT-IRIS parameter in the repair tissue. Thus, the differences in MRI parameters in repair tissue could not be definitively linked with a specific molecular change. Ideally, one would like to obtain a measure of some specific molecular mechanism in a noninvasive, or minimally invasive, manner, so that a targeted therapeutic could be administered.

Differences in the progression of tissue repair were more pronounced in the FT-IRIS analysis, compared to the IFOP analysis. This could be attributable to several factors, including the higher signal to noise ratio of the FT-IRIS

technique, and the lack of influence of the person collecting the data. FT-IRIS, data is collected from a tissue section on a microscope slide in an automated fashion. However, with IFOP data collection, there are several user variables that can influence data quality, including pressure and angle applied, choice of the regions of analysis, and hydration state of the tissue. The IFOP PLS model distinguished repair and normal tissue, but this task was also completed by visual inspection when obtaining the spectra. The PLS model generated for predicting the modified O'Driscoll score from the spectra resulted in an RMSE of 3.59 for the full cross-validation. Considering that the scores used as inputs for the model ranged from 6 to 24, this would only enable a very general prediction of how the repair is progressing, and is not an acceptable model to use for trying to predict the histological score.

Previous studies examined the relationship between IFOP spectra and a Collins visual scale, and a modified Mankin grading scale (0-12) for degenerative cartilage.[29,36,37] There was a correlation with Collins scale, but a stronger correlation with Mankin grade, where the use of IFOP spectra enabled successful prediction of histological score within ±1 grade. The Collins scale is not as complex as the modified O'Driscoll score, and involved only visual assessment of the degraded samples, indicating that visual assessment is not adequate for evaluation of tissue degradation. Perhaps the greatest difference, however, is that the studies focused on degenerative cartilage, consisting of type II collagen, and not repair cartilage, where type I and type II collagen are typically present throughout the depth of the defect. With a more complex tissue, it is possible that the IFOP spectra, which contain information from the surface of the samples only, are not adequate. Near-IR analysis permits assessment deeper into the tissue, up to millimeters, and has been used to assess cartilage degradation[58-63] and repair.[64] However, the absorbances are very broad, dominated by water, and not well defined with respect to specific molecular species,[46,65] so it is not clear whether near-IR alone would be a powerful enough technique to predict a histological grade of repair tissue. Further investigations need to be undertaken to address the true clinical potential of IFOP evaluation of repair cartilage, and should include combined mid-IR and near-IR assessments. This would help elucidate what spectral information is most useful for predicting a tissue grade, and thereby provide useful information for design of therapeutic interventions without the need for biopsy.

Acknowledgments and Funding

The author(s) disclosed receipt of the following financial support for the research, authorship, and/or publication of this article: This work was supported by the National Institutes of Health grant NIH R01 EB000744.

Declaration of Conflicting Interests

The author(s) declared no potential conflicts of interest with respect to the research, authorship, and/or publication of this article.

Ethical Approval

This study was approved by the Hospital for Special Surgery IACUC (Institutional Animal Care and Use Committee).

References

1. Chu CR, Szczodry M, Bruno S. Animal models for cartilage regeneration and repair. Tissue Eng Part B Rev. 2009;16(1):105-15.
2. Johnstone B, Alini M, Cucchiarini M, Dodge GR, Eglin D, Guilak F, *et al*. Tissue engineering for articular cartilage repair—the state of the art. Eur Cell Mater. 2013;25:248-67.
3. Orth P, Cucchiarini M, Kohn D, Madry H. Alterations of the subchondral bone in osteochondral repair—translational data and clinical evidence. Eur Cell Mater. 2013;25:299-316.
4. Simon TM, Aberman HM. Cartilage regeneration and repair testing in a surrogate large animal model. Tissue Eng Part B Rev. 2009;16(1):65-79.
5. Sun H, Liu W, Zhou G, Zhang W, Cui L, Cao Y. Tissue engineering of cartilage, tendon and bone. Front Med. 2011;5(1):61-9.
6. Vaquero J, Forriol F. Knee chondral injuries: clinical treatment strategies and experimental models. Injury. 2011;43(6): 694-705.
7. Yannas IV, Kinner B, Capito RM, Spector M. Regeneration of articular cartilage. In: Regenerative medicine II. Vol. 94. Berlin, Germany: Springer; 2005. p. 129-30.
8. Kamali F, Bayat M, Torkaman G, Ebrahimi E, Salavati M. The therapeutic effect of low-level laser on repair of osteochondral defects in rabbit knee. J Photochem Photobiol B. 2007;88(1):11-5.
9. Virén T, Saarakkala S, Jurvelin JS, Pulkkinen HJ, Tiitu V, Valonen P, *et al*. Quantitative evaluation of spontaneously and surgically repaired rabbit articular cartilage using intra-articular ultrasound method in situ. Ultrasound Med Biol. 2010;36(5):833-9.
10. Hunziker EB. Articular cartilage repair: basic science and clinical progress. A review of the current status and prospects. Osteoarthritis Cartilage. 2002;10(6):432-63.
11. Bae DK, Yoon KH, Song SJ. Cartilage healing after microfracture in osteoarthritic knees. Arthroscopy. 2006;22(4): 367-74.
12. Breinan HA, Martin SD, Hsu HP, Spector M. Healing of canine articular cartilage defects treated with microfracture, a type-II collagen matrix, or cultured autologous chondrocytes. J Orthop Res. 2000;18(5):781-9.
13. Jackson DW, Lalor PA, Aberman HM, Simon TM. Spontaneous repair of full-thickness defects of articular cartilage in a goat model. A preliminary study. J Bone Joint Surg Am. 2001;83(1):53-64.
14. Mainil-Varlet P, Aigner T, Brittberg M, Bullough P, Hollander A, Hunziker E, *et al*. Histological assessment of cartilage

repair: a report by the Histology Endpoint Committee of the International Cartilage Repair Society (ICRS). J Bone Joint Surg Am. 2003;85(Suppl 2):45-57.
15. O'Driscoll SW, Keeley FW, Salter RB. Durability of regenerated articular cartilage produced by free autogenous periosteal grafts in major full-thickness defects in joint surfaces under the influence of continuous passive motion. A follow-up report at one year. J Bone Joint Surg Am. 1988;70(4):595-606.
16. O'Driscoll SW, Keeley FW, Salter RB. The chondrogenic potential of free autogenous periosteal grafts for biological resurfacing of major full-thickness defects in joint surfaces under the influence of continuous passive motion. An experimental investigation in the rabbit. J Bone Joint Surg Am. 1986;68(7):1017-35.
17. Rutgers M, van Pelt MJ, Dhert WJ, Creemers LB, Saris DB. Evaluation of histological scoring systems for tissue-engineered, repaired and osteoarthritic cartilage. Osteoarthritis Cartilage. 2009;18(1):12-23.
18. Coons S, Johnson P, Scheithauer B, Yates A, Pearl D. Improving diagnostic accuracy and interobserver concordance in the classification and grading of primary gliomas. Cancer. 1997;79(7):1381-93.
19. Kozakowski N, Regele H. Biopsy diagnostics in renal allograft rejection: from histomorphology to biological function. Transpl Int. 2009;22(10):945-53.
20. Bi XH, Yang X, Bostrom MPG, Bartusik D, Ramaswamy S, Fishbein KW, *et al*. Fourier transform infrared imaging and MR microscopy studies detect compositional and structural changes in cartilage in a rabbit model of osteoarthritis. Anal Bioanal Chem. 2007;387(5):1601-12.
21. Camacho NP, Carroll P, Raggio CL. Fourier transform infrared imaging spectroscopy (FT-IRIS) of mineralization in bisphosphonate-treated oim/oim mice. Calcif Tissue Int. 2003;72(5):604-9.
22. Camacho NP, West P, Griffith MH, Warren RF, Hidaka C. FT-IR imaging spectroscopy of genetically modified bovine chondrocytes. Mater Sci Eng C Biomim Supramol Syst. 2001;17(1-2):3-9.
23. Camacho NP, West P, Torzilli PA, Mendelsohn R. FTIR microscopic imaging of collagen and proteoglycan in bovine cartilage. Biopolymers. 2001;62(1):1-8.
24. Xia Y, Alhadlaq H, Ramakrishnan N, Bidthanapally A, Badar F, Lu M. Molecular and morphological adaptations in compressed articular cartilage by polarized light microscopy and Fourier-transform infrared imaging. J Struct Biol. 2008;164(1):88-95.
25. Croxford AM, Nandakumar KS, Holmdahl R, Tobin MJ, McNaughton D, Rowley MJ. Chemical changes demonstrated in cartilage by synchrotron infrared microspectroscopy in an antibody-induced murine model of rheumatoid arthritis. J Biomed Opt. 2011;16(6):066004.
26. Kim M, Pugarelli J, Miller TL, Wolfson MR, Dodge GR, Shaffer TH. Brief mechanical ventilation impacts airway cartilage properties in neonatal lambs. Pediatr Pulmonol. 2011;47(8):763-70.
27. Kobrina Y, Rieppo L, Saarakkala S, Pulkkinen HJ, Tiitu V, Valonen P, *et al*. Cluster analysis of infrared spectra can differentiate intact and repaired articular cartilage. Osteoarthritis Cartilage. 2012;21(3):462-9.
28. Rieppo L, Narhi T, Helminen HJ, Jurvelin JS, Saarakkala S, Rieppo J. Infrared spectroscopic analysis of human and bovine articular cartilage proteoglycans using carbohydrate peak or its second derivative. J Biomed Opt. 2013;18(9):97006.
29. Hanifi A, Bi X, Yang X, Kavukcuoglu B, Lin PC, DiCarlo E, *et al*. Infrared fiber optic probe evaluation of degenerative cartilage correlates to histological grading. Am J Sports Med. 2012;40(12):2853-61.
30. Hanifi A, Richardson JB, Kuiper JH, Roberts S, Pleshko N. Clinical outcome of autologous chondrocyte implantation is correlated with infrared spectroscopic imaging-derived parameters. Osteoarthritis Cartilage. 2012;20(9):988-96.
31. Hanifi A, McCarthy H, Roberts S, Pleshko N. Fourier transform infrared imaging and infrared fiber optic probe spectroscopy identify collagen type in connective tissues. PLoS One. 2013;8(5):e64822.
32. Reiter DA, Irrechukwu O, Lin PC, Moghadam S, Von Thaer S, Pleshko N, *et al*. Improved MR-based characterization of engineered cartilage using multiexponential T2 relaxation and multivariate analysis. NMR Biomed. 2012;25(3):476-88.
33. Reiter DA, Roque RA, Lin PC, Doty SB, Pleshko N, Spencer RG. Improved specificity of cartilage matrix evaluation using multiexponential transverse relaxation analysis applied to pathomimetically degraded cartilage. NMR Biomed. 2011;24(10):1286-94.
34. Kim M, Foo LF, Uggen C, Lyman S, Ryaby JT, Moynihan DP, *et al*. Evaluation of early osteochondral defect repair in a rabbit model utilizing Fourier transform-infrared imaging spectroscopy, magnetic resonance imaging, and quantitative T2 mapping. Tissue Eng Part C Methods. 2010;16(3):355-64.
35. Masahiko T, Damle S, Penmatsa M, West P, Yang X, Bostrom M, *et al*. Temporal changes in collagen cross-links in spontaneous articular cartilage repair. Cartilage. 2012;3(3):278-87.
36. Li G, Thomson M, Dicarlo E, Yang X, Nestor B, Bostrom MP, *et al*. A chemometric analysis for evaluation of early-stage cartilage degradation by infrared fiber-optic probe spectroscopy. Appl Spectrosc. 2005;59(12):1527-33.
37. West PA, Bostrom MPG, Torzilli PA, Camacho NP. Fourier transform infrared spectral analysis of degenerative cartilage: an infrared fiber optic probe and imaging study. Appl Spectrosc. 2004;58(4):376-81.
38. Fischer AH, Jacobson KA, Rose J, Zeller R. Hematoxylin and eosin staining of tissue and cell sections. CSH Protoc. 2008;2008:pdb.prot4986.
39. Landis JR, Koch GG. Measurement of observer agreement for categorical data. Biometrics. 1977;33(1):159-74.
40. Bi X, Li G, Doty SB, Camacho NP. A novel method for determination of collagen orientation in cartilage by Fourier transform infrared imaging spectroscopy (FT-IRIS). Osteoarthritis Cartilage. 2005;13(12):1050-8.
41. Gadaleta SJ, Landis WJ, Boskey AL, Mendelsohn R. Polarized FT-IR microscopy of calcified turkey leg tendon. Connect Tissue Res. 1996;34(3):203-11.
42. Bi XH, Yang X, Bostrom MPG, Camacho NP. Fourier transform infrared imaging spectroscopy investigations in the pathogenesis and repair of cartilage. Biochim Biophys Acta. 2006;1758(7):934-41.

43. Boskey A, Pleshko Camacho N. FT-IR imaging of native and tissue-engineered bone and cartilage. Biomaterials. 2007;28(15):2465-78.
44. West PA, Torzilli PA, Chen C, Lin P, Camacho NP. Fourier transform infrared imaging spectroscopy analysis of collagenase-induced cartilage degradation. J Biomed Opt. 2005;10(1):14015.
45. Geladi P, Kowalski BR. Partial least-squares regression—a tutorial. Anal Chim Acta. 1986;185:1-17.
46. Padalkar M, Spencer R, Pleshko N. Near infrared spectroscopic evaluation of water in hyaline cartilage. Ann Biomed Eng. 2013;41(11):2426-36.
47. Lasch P, Schmitt J, Beekes M, Udelhoven T, Eiden M, Fabian H, *et al*. Antemortem identification of bovine spongiform encephalopathy from serum using infrared spectroscopy. Anal Chem. 2003;75(23):6673-8.
48. Terajima M, Damle S, Penmatsa M, West P, Yang X, Bostrom M, *et al*. Temporal changes in collagen cross-links in spontaneous articular cartilage repair. Cartilage. 2012;3(3):278-87.
49. Julkunen P, Harjula T, Iivarinen J, Marjanen J, Seppanen K, Narhi T, *et al*. Biomechanical, biochemical and structural correlations in immature and mature rabbit articular cartilage. Osteoarthritis Cartilage. 2009;17(12):1628-38.
50. Kiviranta I, Jurvelin J, Tammi M, Saamanen AM, Helminen HJ. Microspectrophotometric quantitation of glycosaminoglycans in articular-cartilage sections stained with safranin-O. Histochemistry. 1985;82(3):249-55.
51. Olofsson LB, Svensson O, Lorentzon R, Lindstrom I, Alfredson H. Periosteal transplantation to the rabbit patella. Knee Surg Sports Traumatol Arthrosc. 2007;15(5):560-3.
52. Goebe L, Orth P, Muller A, Zurakowsk D, Bucker A, Cucchiarini M, *et al*. Experimental scoring systems for macroscopic articular cartilage repair correlate with the MOCART score assessed by a high-field MRI at 9.4 T—comparative evaluation of five macroscopic scoring systems in a large animal cartilage defect model. Osteoarthritis Cartilage. 2012;20(9):1046-55.
53. Chang N, Lam C, Lin C, Chen W, Li C, Lin Y, *et al*. Transplantation of autologous endothelial progenitor cells in porous PLGA scaffolds create a microenvironment for the regeneration of hyaline cartilage in rabbits. Osteoarthritis Cartilage. 2013;21(10):1613-22.
54. Fortier L, Potter H, Rickey E, Schnabel L, Foo L, Chong L, *et al*. Concentrated bone marrow aspirate improves full-thickness cartilage repair compared with microfracture in the equine model. J Bone Joint Surg Am. 2010;92(10):1927-37.
55. Watanabe A, Boesch C, Anderson S, Brehm W, Mainil Varlet P. Ability of dGEMRIC and T2 mapping to evaluate cartilage repair after microfracture: a goat study. Osteoarthritis Cartilage. 2009;17(10):1341-9.
56. Watrin-Pinzano A, Ruaud JP, Cheli Y, Gonord P, Grossin L, Bettembourg-Brault I, *et al*. Evaluation of cartilage repair tissue after biomaterial implantation in rat patella by using T2 mapping. MAGMA. 2004;17(3-6):219-28.
57. Nieminen MT, Rieppo J, Toyras J, Hakumaki JM, Silvennoinen J, Hyttinen MM, *et al*. T2 relaxation reveals spatial collagen architecture in articular cartilage: a comparative quantitative MRI and polarized light microscopic study. Magn Reson Med. 2001;46(3):487-93.
58. Afara I, Prasadam I, Moody H, Crawford R, Xiao Y, Oloyede A. Near infrared spectroscopy for rapid determination of Mankin score components: a potential tool for quantitative characterization of articular cartilage at surgery. Arthroscopy. 2014;30(9):1146-55.
59. Stumpfe S, Pester J, Steinert S, Marintschev I, Plettenberg H, Aurich M, *et al*. Is there a correlation between biophotonical, biochemical, histological, and visual changes in the cartilage of osteoarthritic knee-joints? Muscles. 2013;3(3):157-65.
60. Spahn G, Felmet G, Hofmann G. Traumatic and degenerative cartilage lesions: arthroscopic differentiation using near-infrared spectroscopy (NIRS). Arch Orthop Trauma Surg. 2013;133(7):997-1002.
61. Brown C, Jayadev C, Glyn-Jones S, Carr A, Murray D, Price A, *et al*. Characterization of early stage cartilage degradation using diffuse reflectance near infrared spectroscopy. Phys Med Biol. 2011;56(7):2299-307.
62. Hofmann G, Marticke J, Grossstuck R, Hoffmann M, Lange M, Plettenberg H, *et al*. Detection and evaluation of initial cartilage pathology in man: a comparison between MRT, arthroscopy and near-infrared spectroscopy (NIR) in their relation to initial knee pain. Pathophysiology. 2009;17(1):1-8.
63. Spahn G, Plettenberg H, Nagel H, Kahl E, Klinger H, Muckley T, *et al*. Evaluation of cartilage defects with near-infrared spectroscopy (NIR): an ex vivo study. Med Eng Phys. 2008;30(3):285-92.
64. Guenther D, Liu C, Horstmann H, Krettek C, Jagodzinski M, Haasper C. Near-infrared spectroscopy correlates with established histological scores in a miniature pig model of cartilage regeneration. Open Orthop J. 2014;8:93-9.
65. Palukuru U, McGoverin C, Pleshko N. Assessment of hyaline cartilage matrix composition using near infrared spectroscopy. Matrix Biol. 2014;38:3-11.